Environmental Science Nano

PAPER

Cite this: *Environ. Sci.: Nano*, 2017, **4**, 720

Understanding enzymatic degradation of single-walled carbon nanotubes triggered by functionalization using molecular dynamics simulation

Ming Chen,*[ab] Guangming Zeng,*[ab] Piao Xu,[ab] Yi Zhang,[ab] Danni Jiang[ab] and Shuang Zhou[ab]

Received 16th January 2017,
Accepted 1st February 2017

DOI: 10.1039/c7en00050b

rsc.li/es-nano

Enzymes are promising candidates for removing environmental carbon nanotubes (CNTs). However, pristine CNTs are difficult to degrade by plant or animal enzymes, such as horseradish peroxidase (HRP) and lactoperoxidase (LPO), and functionalization is often needed for CNT biodegradation. By constructing 12 systems comprising two well-known CNT-degrading enzymes (HRP and LPO) with or without carboxylated or pristine single-walled CNTs (SWCNTs), we answer questions as to how functionalization changes the energetic properties and enzymatic conformations to facilitate the occurrence of SWCNT degradation and how these analysed enzymes respond to different carboxylated SWCNTs using molecular dynamics (MD) simulations. Significant conformational changes in the enzymes were found after the SWCNTs were carboxylated, and functionalization improved the structural stability of enzyme–substrate complexes. Numerous carboxylated SWCNTs induced a similar variation trend of global conformations for both HRP and LPO at the late stages, but their cavity volumes showed totally different change patterns with time. Our study provides a molecular-level understanding of functionalization's roles in SWCNT biodegradation and a molecular basis to develop more biocompatible and biodegradable CNTs.

Environmental significance

Carbon nanotubes (CNTs), as widely applied nanomaterials, exhibit adverse impacts on living organisms and the environment. Thus, their efficient removal from the environment is becoming increasingly important. CNT degradation by plant or animal enzymes is a good method to achieve this purpose, and CNT functionalization is often needed before degradation. However, the molecular basis for the enzymatic degradation of CNTs triggered by functionalization has been unclear until now. Here, we explored this molecular basis based on two known CNT-degrading enzymes with pristine and carboxylated single-walled CNTs (SWCNTs), and show that functionalized SWCNTs lead to a more stable interaction between the degrading enzymes and their substrates than pristine ones because of conformation transformations. Different SWCNTs induced completely inconsistent cavity volume change patterns of their degrading enzymes with time.

Introduction

The interest in biodegradation of carbon nanotubes (CNTs) has grown significantly in the past years due to numerous studies reporting their potential negative impacts on the environment and the ecosystem,[1–4] although CNTs are also reported to provide benefits to environmental remediation.[5–7] It is believed that biodegradation is one of the good options to deal with the risks of CNTs and other pollutants.[8–12]

Biodegradation of CNTs mainly relies on various enzymes, *e.g.* horseradish peroxidase (HRP) and lactoperoxidase (LPO).[13,14] Functionalization is often necessary for CNT biodegradation by plant or animal enzymes. Microbial enzymes can be exceptions, because there has been a study that reported microbial enzymatic degradation of pristine single-walled carbon nanotubes (SWCNTs).[15] Surface functionalization with coumarin derivatives and catechol accelerated the HRP-mediated CNT degradation compared to simply oxidized CNTs.[8] Surface modification also produces CNTs with better biocompatibility and faster biodegradability *in vivo* in mice.[16] Several research groups have observed the degradation of oxidized CNTs by myeloperoxidase.[17–19] The molecular basis of pristine SWCNT degradation by a

[a] *College of Environmental Science and Engineering, Hunan University, Changsha 410082, China. E-mail: mchensn@hnu.edu.cn, zgming@hnu.edu.cn*
[b] *Key Laboratory of Environmental Biology and Pollution Control, Hunan University, Ministry of Education, Changsha 410082, China*

microbial enzyme has been solved recently, showing that free conformational transformation in the enzyme is important for the degradation of SWCNT by manganese peroxidase (MnP) from *Phanerochaete chrysosporium*.[9]

However, the molecular-level basis related to enzymatic degradation of CNTs induced by functionalization has been still poorly understood until now. There are still two problems to be solved: (i) how does functionalization change the energetic properties and enzymatic conformations to facilitate the occurrence of SWCNT degradation? (ii) How do the degrading enzymes respond to different functionalized SWCNTs?

In this study, five molecular dynamics (MD) simulations for HRP and five MD simulations for LPO in interaction with pristine and carboxylated SWCNTs were performed. Two additional MD simulations without SWCNTs (one for HRP and one for LPO) were also run for comparison purposes. A total of five SWCNTs are adopted (Fig. 1a), where one is pristine and the remaining are carboxylated.

(a)

CNT	n	m	No. of unit cells	Length (Å)	Radius (Å)	Type
p-SWCNT-(5,5,2)	5	5	2	4.91	3.39	Pristine
o-SWCNT-(5,5,2)	5	5	2	4.91	3.39	Carboxylated
o-SWCNT-(5,5,3)	5	5	3	7.37	3.39	Carboxylated
o-SWCNT-(5,5,4)	5	5	4	9.82	3.39	Carboxylated
o-SWCNT-(5,4,2)	5	4	2	66.45	3.05	Carboxylated

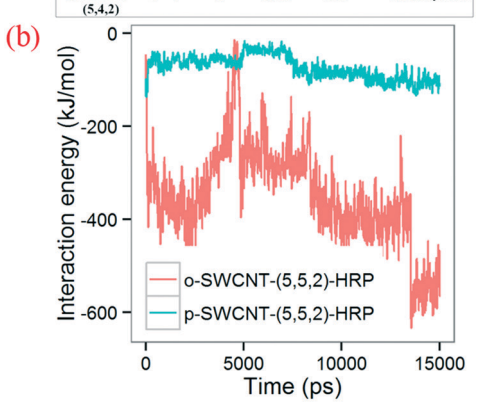

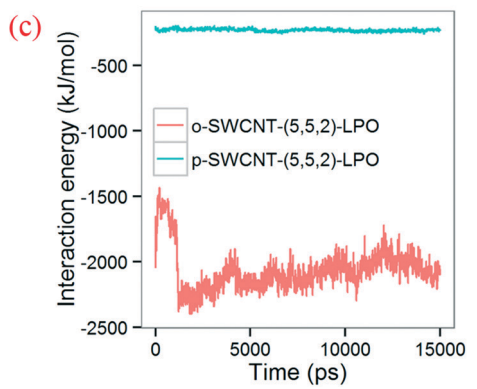

Fig. 1 (a) Selected five SWCNTs. (b) Interaction energies between HRP and SWCNTs. (c) Interaction energies between LPO and SWCNTs.

Materials and methods

Five types of SWCNTs were used in the present study (Fig. 1), including (5,5)- and (5,4)-SWCNTs. Among these SWCNTs, four are (5,5)-SWCNTs in different lengths with or without terminal carboxylation and one is (5,4)-SWCNTs with terminal carboxylation. The structures of two well-known SWCNT-degrading enzymes (HRP and LPO) were obtained from the Protein Data Bank:[20] 1H55 (ref. 21) for HRP and 3BXI[22] for LPO. The HRP structure has been solved to 1.61 Å resolution with 308 amino acids; whereas the 3D structure of LPO is at 2.3 Å with 595 amino acids. Their cofactors and water molecules were deleted.

The above-mentioned five SWCNTs were bound to each of these two degrading enzymes by PatchDock[23] + FireDock[24] software, as was done in our previous studies.[2,9] A total of ten optimized complexes were produced for further MD simulations. For simplicity, the pristine SWCNT was called p-SWCNT, while the carboxylated SWCNT was called o-SWCNT. The SWCNT-(n,m) composed of x unit cells was named SWCNT-(n,m,x). Thus, the 10 complexes are p-SWCNT-(5,5,2)-HRP, p-SWCNT-(5,5,2)-LPO, o-SWCNT-(5,5,2)-HRP, o-SWCNT-(5,5,2)-LPO, o-SWCNT-(5,5,3)-HRP, o-SWCNT-(5,5,3)-LPO, o-SWCNT-(5,5,4)-HRP, o-SWCNT-(5,5,4)-LPO, o-SWCNT-(5,4,2)-HRP, and o-SWCNT-(5,4,2)-LPO. To facilitate the comparison, two SWCNT-free structures for HRP and LPO ($HRP_{no\text{-}SWCNT}$ and $LPO_{no\text{-}SWCNT}$) were also constructed, respectively.

Consistent with our previous studies,[2,9] the OPLS-AA force field[25] and SPC water model[26] were selected. Cl^- or Na^+ was used to neutralize the above 12 systems after solvation: 1 Na^+ and 15 484 water molecules for p-SWCNT-(5,5,2)-HRP; 8 Cl^- and 30 752 water molecules for p-SWCNT-(5,5,2)-LPO; 21 Na^+ and 15 449 water molecules for o-SWCNT-(5,5,2)-HRP; 12 Na^+ and 30 732 water for o-SWCNT-(5,5,2)-LPO; 21 Na^+ and 15 444 water for o-SWCNT-(5,5,3)-HRP; 12 Na^+ and 30 724 water molecules for o-SWCNT-(5,5,3)-LPO; 21 Na^+ and 15 429 water molecules for o-SWCNT-(5,5,4)-HRP; 12 Na^+ and 30 715 water molecules for o-SWCNT-(5,5,4)-LPO; 19 Na^+ and 33 240 water molecules for o-SWCNT-(5,4,2)-HRP; 10 Na^+ and 43 317 water molecules for o-SWCNT-(5,4,2)-LPO; 1 Na^+ and 15 523 water molecules for $HRP_{no\text{-}SWCNT}$; 8 Cl^- and 30 771 water molecules for $LPO_{no\text{-}SWCNT}$. Then, the systems were treated using the steepest descent minimization algorithm under periodic boundary conditions. The energy step size is set to 0.01 nm. Then, we carried out pre-equilibration of the systems in 0.5 ns NVT + 0.5 ns NPT ensembles. Twelve MD simulations were run at 300 K and 1 bar by means of the GROMACS software package (version 4.60)[27] for these systems. For each MD simulation, 15 ns was employed. This simulated time length was found to be enough for the purpose of the present study. We set the time step to 2 fs and saved the results every 10 ps. The analyses and calculations were performed based on the produced MD trajectories.

The global conformation variations in the enzymes were analyzed using the solvent accessible surface area (S) and backbone RMSD. The local conformational dynamics was

described by focusing on the cavity volumes of HRP and LPO and the number of solvent molecules overlapping the cavities of the enzyme ($N_{solvent}$). These two variables were calculated by trj_cavity[28] which can fast detect the protein cavities within MD trajectories.

The interaction energy between five SWCNTs and each of the two selected degrading enzymes (HPR and LPO) was analyzed, respectively, by using the following formula:

$$E_{interaction} = E_{LJ\text{-}SR} + E_{C\text{-}SR}$$

where $E_{interaction}$ is the interaction energy between a SWCNT and its degrading enzyme; $E_{LJ\text{-}SR}$ is the short-range Lennard-Jones energy of the complex composed of a SWCNT and its degrading enzyme; and $E_{C\text{-}SR}$ is the short-range Coulomb energy of the SWCNT–enzyme interaction.

Results and discussion

Functionalized SWCNTs induce more stable interaction between enzymes and substrates than pristine SWCNTs

Pristine CNTs are generally difficult to degrade by animal and plant enzymes.[14,29] Functionalization can change the CNT properties, allowing the degradation to occur or be enhanced.[8] It is still unclear why functionalization is able to lead to enzymatic degradation of CNTs at the molecular level. Here, we employed MD simulations to investigate the potential molecular mechanism of functionalization-caused enzymatic degradation of SWCNTs based on two known SWCNT-degrading enzymes (HRP and LPO). In this study, functionalization refers to the carboxylation of the SWCNTs. The functionalization of CNTs by carboxylation is the most frequently used method to modify the CNT properties in previous studies related to their biodegradation.[13,30,31] This is because CNTs modified with carboxyl groups are believed to be more easily attacked by enzymes than those with other groups.[14,29] In general, oxidation is a precondition for the SWCNT degradation by HRP[8,13,32] and LPO.[14] Pristine and carboxylated SWCNTs, *i.e.*, p-SWCNT-(5,5,2) and o-SWCNT-(5,5,2), were selected to evaluate the effect of carboxylation on the energetic and conformational properties of HRP and LPO with time. o-SWCNT-(5,5,2) was produced by introducing the carboxyl groups at both ends of the SWCNT. The reason that we selected SWCNT-(5,5) for our study is because this SWCNT is extensively adopted in previous experimental or simulation studies.[33–37] The complexes of SWCNTs with their degrading enzymes (HRP and LPO) were produced by molecular docking which has also been used to characterize the interactions between eosinophil peroxidase and SWCNTs[31] as well as between myeloperoxidase and SWCNTs.[17] MD simulations for the systems with p-SWCNT-(5,5,2) and o-SWCNT-(5,5,2) were set to the same conditions. The method used in the present study, MD simulation, has been proven reliable for exploring protein–nanomaterial interactions.[2,9,38–41]

To observe the structural stability of SWCNT–enzyme complexes, we calculated the interaction energies between the SWCNT and the enzyme. The smaller the interaction energy, the more stable the complex structure.[9,34] The average interaction energy between p-SWCNT-(5,5,2) and HRP is −73.539 kJ mol^{-1}, while that between o-SWCNT-(5,5,2) and HRP is −350.574 kJ mol^{-1} (Fig. 1b). This showed that carboxylation of the SWCNT largely decreased the interaction energy between the HRP and its substrate, significantly enhancing the structural stability of the enzyme–substrate complex. The same is true for LPO and the SWCNT, where the interaction energy between them had a bigger reduction on average from −226.735 to −2069.34 kJ mol^{-1} due to carboxylation (Fig. 1c).

Enhancement of the structural stability of an enzyme–substrate complex by carboxylation may be an important mechanism for SWCNT degradation by plant or animal enzymes. Our previous study showed that there is a large conformational change in SWCNT–degrading enzyme.[9] Recently, we have found that SWCNT release has an effect on the biodegradation processes of polycyclic aromatic hydrocarbons (PAHs), β-hexachlorocyclohexane and lignin model compounds by affecting the conformational dynamics of enzyme structures.[2] Functionalized SWCNTs may induce beneficial conformations in HRP or LPO to degrade the SWCNT, while pristine SWCNTs cannot.

Next, we differentiate the degree of enzymatic conformational change between the complexes with pristine and carboxylated SWCNTs. Thus, we defined the following several variables:

$$RD = |RMSD_{SWCNT\text{-}EN} - RMSD_{free}|$$

$$SD = |SASA_{SWCNT\text{-}EN} - SASA_{free}|$$

$$VD = |Volume_{SWCNT\text{-}EN} - Volume_{free}|$$

where RD, SD and VD are the absolute values of the differences between backbone RMSDs, S and cavity volumes of the enzyme in the presence and absence of SWCNTs, respectively; $RMSD_{SWCNT\text{-}EN}$, $SASA_{SWCNT\text{-}EN}$ and $Volume_{SWCNT\text{-}EN}$ are the backbone RMSD, S and cavity volume of the enzyme with SWCNTs, respectively; $RMSD_{free}$, $SASA_{free}$ and $Volume_{free}$ are the backbone RMSD, S and cavity volume of the enzyme without SWCNTs, respectively.

Our results showed that there was a significant difference in RD between p-SWCNT-(5,5,2)-HRP and o-SWCNT-(5,5,2)-HRP ($p < 0.05$) (Fig. 2A) as well as between p-SWCNT-(5,5,2)-LPO and o-SWCNT-(5,5,2)-LPO ($p < 0.01$) (Fig. 3A). This means that pristine and carboxylated SWCNTs cause significantly different backbone fluctuations in HRP and LPO. The o-SWCNT-(5,5,2) induced a larger mean SD than p-SWCNT-(5,5,2) for HRP (4.2 *vs.* 3.0, $t = 16.7243$, $p < 0.01$) (Fig. 2B), whereas the tendency was opposite for LPO (5.0 *vs.* 8.0, $t = -24.5409$, $p < 0.01$) (Fig. 3B). Thus, the SWCNT has led to a significant change in S of its degrading enzymes. Interestingly, mean VD was also found to be larger for o-SWCNT-(5,5,2)-

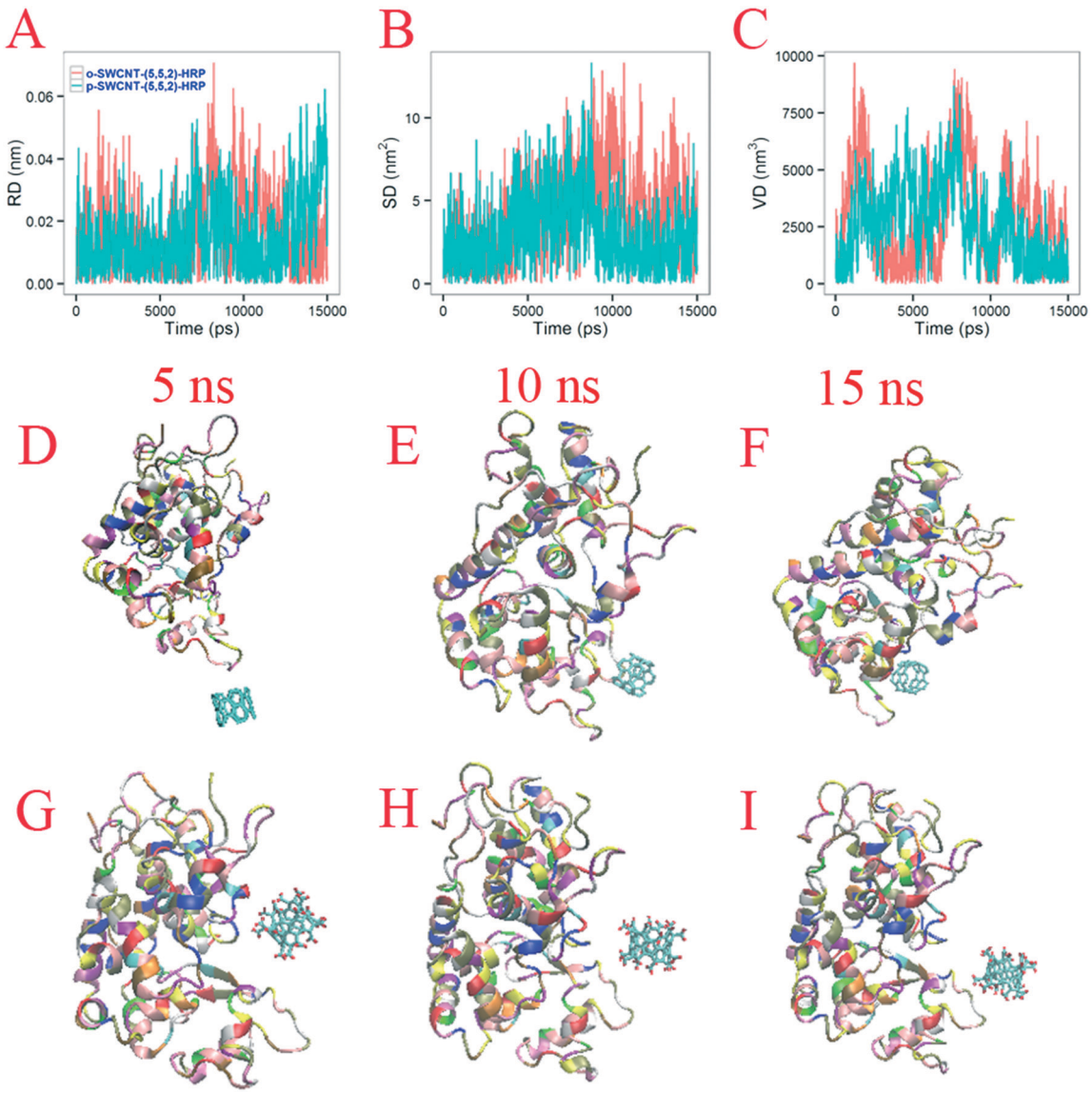

Fig. 2 The time-dependent RD (A), SD (B) and VD (C) of HRP in the presence of p-SWCNT-(5,5,2) and o-SWCNT-(5,5,2). D–F, snapshots of p-SWCNT-(5,5,2)-HRP at 5, 10 and 15 ns. G–I, snapshots of o-SWCNT-(5,5,2)-HRP at 5, 10 and 15 ns.

HRP than for p-SWCNT-(5,5,2)-HRP ($p < 0.01$) (Fig. 2C), and smaller for o-SWCNT-(5,5,2)-LPO than for p-SWCNT-(5,5,2)-LPO (Fig. 3C). The initial cavity volume of HRP without SWCNTs is 22 695.62 nm^3. The appearance of o-SWCNT-(5,5,2) leads to an increase in the cavity volume of HRP by 565.264 nm^3. By contrast, this volume was decreased by p-SWCNT-(5,5,2) by 200.312 nm^3. However, changes in the cavity volume of HRP with p-SWCNT-(5,5,2) and o-SWCNT-(5,5,2) did not follow this initial trend, given that this volume could increase or decrease at the next stages. Consistent with RD and SD, VD exhibited a significant difference between p-SWCNT-(5,5,2)-HRP and o-SWCNT-(5,5,2)-HRP ($p < 0.01$) as well as between p-SWCNT-(5,5,2)-LPO and o-SWCNT-(5,5,2)-LPO ($p < 0.01$). On average, p-SWCNT-(5,5,2) caused a change in cavity volume of 2614 nm^3 for HRP and 7642 nm^3 for LPO. Unlike this pristine SWCNT, o-SWCNT-(5,5,2) resulted in a change in cavity volume of 2924 nm^3 for HRP and 4173 nm^3 for LPO. To take a more careful look at the conformational variations in HRP and LPO, we extracted three snapshots for each of them at 5, 10 and 15 ns (Fig. 2D–I for HRP and Fig. 3D–I for LPO). Clearly, the conformations of HRP or LPO with the pristine SWCNT at 5, 10 and 15 ns are completely different from those of HRP or LPO with carboxylated SWCNTs, respectively. This further confirms the above findings that the carboxylated and pristine SWCNTs caused significantly different conformational transitions in the enzymes. The induced conformational transitions in HRP or LPO by carboxylation make their binding to the SWCNT firmer.

In short, a significantly different conformational transformation pattern in the SWCNT–degrading enzymes was observed after carboxylation, which may act as the molecular

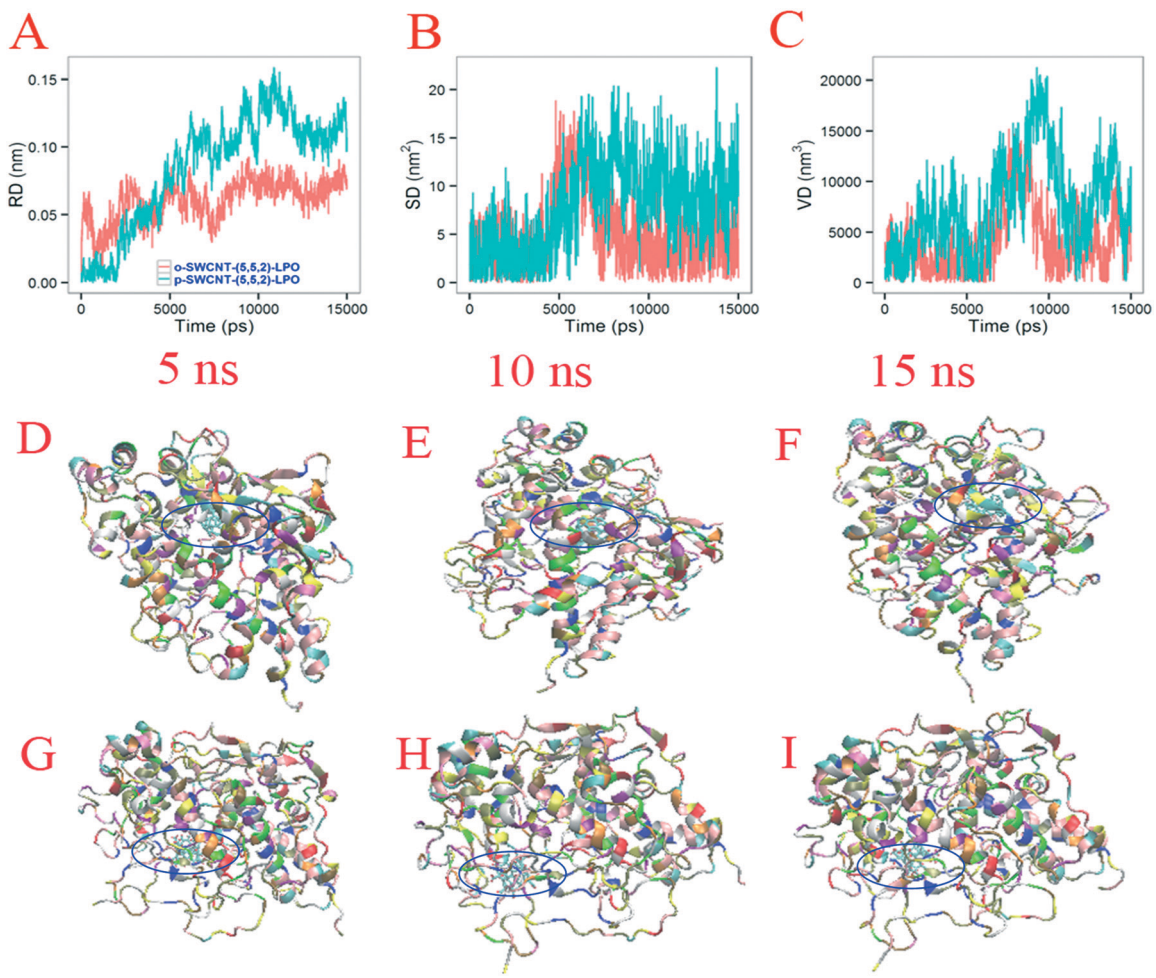

Fig. 3 The time-dependent RD (A), SD (B) and VD (C) of LPO in the presence of p-SWCNT-(5,5,2) and o-SWCNT-(5,5,2). D–F, snapshots of p-SWCNT-(5,5,2)-LPO at 5, 10 and 15 ns. G–I, snapshots of o-SWCNT-(5,5,2)-LPO at 5, 10 and 15 ns.

basis of functionalization-triggered enzymatic degradation. Functionalization may lead to a better interaction between the enzyme and its substrate[8] by conformation transformation. Overall, HRP and LPO showed opposite interaction modes with pristine and carboxylated SWCNTs, *i.e.*, oxidized SWCNTs generally induced larger conformational transformation in HRP than the pristine one, and that is just the opposite for LPO. This may be due to their different structural flexibilities in adapting to the shapes of pristine and carboxylated SWCNTs. Thus, the occurrence of beneficial conformational changes to SWCNT degradation is enzyme-dependent.

How do functionalization's effects on enzymatic conformations vary with different carboxylated SWCNTs?

A variety of studies have reported the key roles of functionalization in enzymatic degradation of CNTs.[8,14,32] Functionalization's effects on enzymatic conformations may vary with different SWCNTs during their degradation. In this study, four different carboxylated SWCNTs, *i.e.* o-SWCNT-(5,5,2), o-SWCNT-(5,5,3), o-SWCNT-(5,5,4) and o-SWCNT-(5,4,2) of different chiralities, lengths, or radii, were chosen to explore this issue. Several previous studies have shown that the properties of the CNTs are influenced by the chirality, such as mechanical[42] and exciton[43] properties. The difference in the properties of CNTs caused by the chirality may affect their interactions with degrading enzymes. Thus, in this study, we selected multiple SWCNTs with different chiralities. We further employed RMSD and S to reflect the global conformational changes in the SWCNT–degrading enzyme, and used the cavity volume and $N_{solvent}$ to observe the local conformational changes in the SWCNT–degrading enzyme. RMSD and S are two frequently used variables to describe conformational changes in proteins.[38,41]

Fig. 4 displays the changes in HRP conformation by different SWCNTs with the same chirality (o-SWCNT-(5,5,2), o-SWCNT-(5,5,3) and o-SWCNT-(5,5,4)) or with the same cell sizes (o-SWCNT-(5,5,2) and o-SWCNT-(5,4,2)). Overall, the trends for RMSD and S of HRP in the presence of these SWCNTs were similar with time, respectively (Fig. 4A and B). Interestingly, the $N_{solvent}$ of HRP was nearly the same in the presence of SWCNTs with the same chirality (n = 5, m = 5), and this number increased when the chiral index m of the SWCNT became four (Fig. 4D). The range of cavity volumes

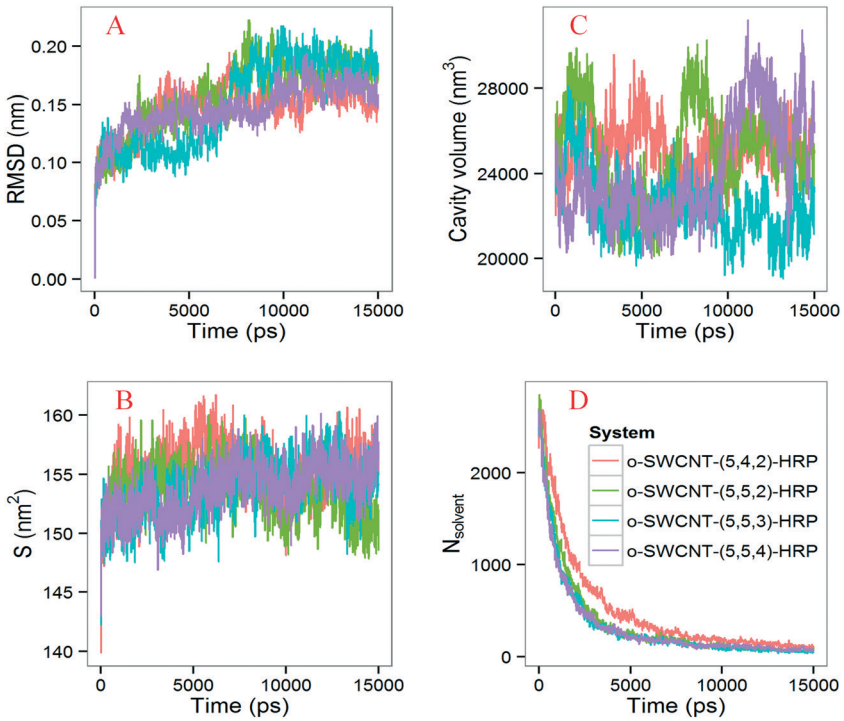

Fig. 4 The effects of different carboxylated SWCNTs on HRP. A, RMSD; B, the solvent accessible surface area (*S*); C, cavity volume; D, $N_{solvent}$.

of HRP during the whole simulation time was 20 097.06–30 271.81 nm^3 for o-SWCNT-(5,5,2), 19 073.54–28 101.3 nm^3 for o-SWCNT-(5,5,3), 20 011.99–31 210.26 nm^3 for o-SWCNT-(5,5,4) and 21 663.88–29 572.09 nm^3 for o-SWCNT-(5,4,2) (Fig. 4C). Thus, the o-SWCNT-(5,4,2) with a smaller chiral index than o-SWCNT-(5,5,2), o-SWCNT-(5,5,3) and o-SWCNT-(5,5,4) allowed fewer volume changes in HRP. The cavity volume of HRP was largely affected by these SWCNTs, given that different SWCNTs induced completely inconsistent volume change patterns with time.

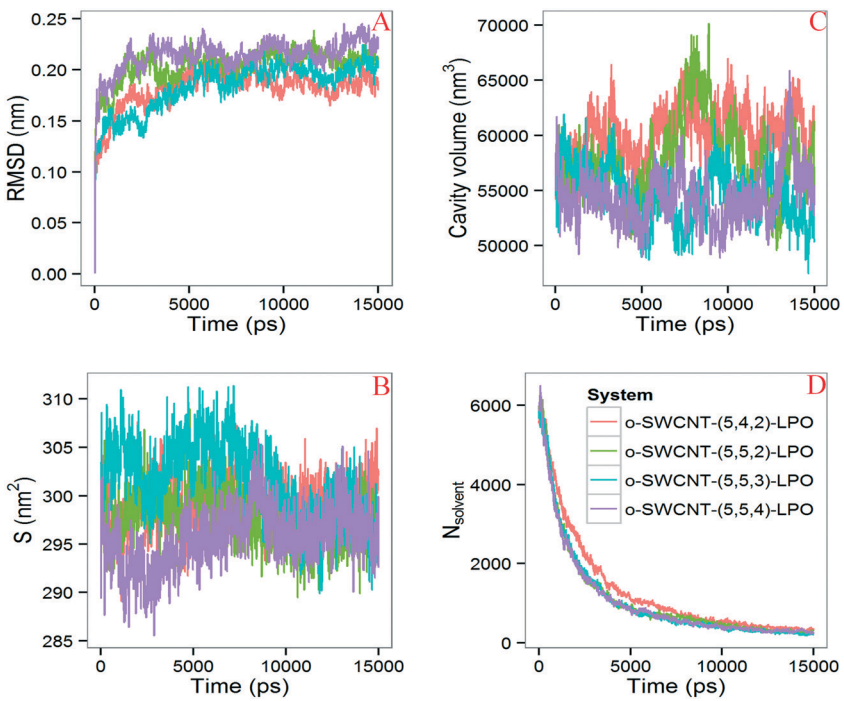

Fig. 5 The effects of different carboxylated SWCNTs on LPO. A, RMSD; B, the solvent accessible surface area (*S*); C, cavity volume; D, $N_{solvent}$.

The trends for LPO with respect to RMSD, *S* and cavity volume are somewhat different from those for HRP, respectively. The RMSD and *S* of LPO showed obvious deviation between the systems with different SWCNTs before about 7 ns (Fig. 5A and B). However, the trends for RMSD and *S* of LPO became similar between different systems after about 7 ns, respectively. However, the rule for the change in $N_{solvent}$ of LPO is almost completely consistent with that of HRP (Fig. 5D). That is, the cell sizes nearly had no effects on the $N_{solvent}$, but the chirality variation from 5 to 4 made more solvent molecules occupy the cavities of LPO. The cavity volume dramatically fluctuated with time for all analysed systems with a variety of SWCNTs (Fig. 5C). LPO showed totally different cavity change patterns between all these systems. Therefore, the main effect of different SWCNTs on LPO is also the change in its cavity volume, which is similar to HRP.

Taking these results together, we can find that different SWCNTs would lead to global conformational changes in the degrading enzymes (HRP and LPO) as reflected by RMSD and *S*, and finally the global conformational changes would show a similar trend with time. The interactional changes between all investigated systems can be due to different properties of SWCNTs, because a previous study showed that the interaction between CNTs and other molecules was related to the CNT properties.[44] Zhao *et al.*[45] reported that features of CNTs, such as the diameter and surface, impacted on the interaction between CNTs and the bovine serum albumin (BSA) protein. CNTs with smaller diameters resulted in a greater decrease in stability of the BSA protein. As for local conformations of SWCNT-degrading enzymes, they would be largely influenced by various SWCNTs with completely different variation trends, as reflected by the enzymatic cavities which are very important in enzymatic functions (*e.g.* substrate binding and enzymatic catalysis).[28]

Conclusions

We have investigated the potential molecular basis of functionalization-triggered SWCNT degradation by plant and animal enzymes. The main findings include: (1) carboxylation enhances the structural stability of enzyme–substrate complexes; (2) the conformational transitions in SWCNT-degrading enzymes with the carboxylated SWCNT are significantly different from those with the pristine SWCNT; (3) the appearance of beneficial conformations to SWCNT degradation is enzyme-dependent; and (4) different carboxylated SWCNTs induce distinctive cavity change patterns. This study provides a molecular basis to design safe carbon nanomaterials that can be easily removed from the environment.

Acknowledgements

The study was financially supported by the National Natural Science Foundation of China (51508177, 51521006, and 51378190), and the Program for Changjiang Scholars and Innovative Research Team in University (IRT-13R17).

Notes and references

1 M. Chen, X. Qin and G. Zeng, *Trends Biotechnol.*, 2017, DOI: 10.1016/j.tibtech.2016.1012.1001.
2 M. Chen, X. Qin and G. Zeng, *Chemosphere*, 2016, **163**, 217–226.
3 P. Wick, M. J. Clift, M. Rösslein and B. Rothen-Rutishauser, *ChemSusChem*, 2011, **4**, 905–911.
4 K. Bhattacharya, F. T. Andón, R. El-Sayed and B. Fadeel, *Adv. Drug Delivery Rev.*, 2013, **65**, 2087–2097.
5 W.-W. Tang, G.-M. Zeng, J.-L. Gong, J. Liang, P. Xu, C. Zhang and B.-B. Huang, *Sci. Total Environ.*, 2014, **468**, 1014–1027.
6 W.-W. Tang, G.-M. Zeng, J.-L. Gong, Y. Liu, X.-Y. Wang, Y.-Y. Liu, Z.-F. Liu, L. Chen, X.-R. Zhang and D.-Z. Tu, *Chem. Eng. J.*, 2012, **211**, 470–478.
7 C. Zhang, C. Lai, G. Zeng, D. Huang, C. Yang, Y. Wang, Y. Zhou and M. Cheng, *Water Res.*, 2016, **95**, 103–112.
8 A. R. Sureshbabu, R. Kurapati, J. Russier, C. Ménard-Moyon, I. Bartolini, M. Meneghetti, K. Kostarelos and A. Bianco, *Biomaterials*, 2015, **72**, 20–28.
9 M. Chen, X. Qin, J. Li and G. Zeng, *RSC Adv.*, 2016, **6**, 3592–3599.
10 D. L. Huang, G. Zeng, C. L. Feng, S. Hu, X. Y. Jiang, L. Tang, F. F. Su, Y. Zhang, W. Zeng and H. L. Liu, *Environ. Sci. Technol.*, 2008, **42**, 4946–4951.
11 L. Tang, G. Zeng, G. L. Shen, Y. P. Li, Y. Zhang and D. L. Huang, *Environ. Sci. Technol.*, 2008, **42**, 1207–1212.
12 M. Chen, P. Xu, G. Zeng, C. Yang, D. Huang and J. Zhang, *Biotechnol. Adv.*, 2015, **33**, 745–755.
13 D. X. Flores-Cervantes, H. M. Maes, A. Schäffer, J. Hollender and H.-P. E. Kohler, *Environ. Sci. Technol.*, 2014, **48**, 4826–4834.
14 K. Bhattacharya, R. El-Sayed, F. T. Andón, S. P. Mukherjee, J. Gregory, H. Li, Y. Zhao, W. Seo, A. Fornara, B. Brandner, M. S. Toprak, K. Leifer, A. Star and B. Fadeel, *Carbon*, 2015, **91**, 506–517.
15 C. Zhang, W. Chen and P. J. Alvarez, *Environ. Sci. Technol.*, 2014, **48**, 7918–7923.
16 D. Mata, M. Amaral, A. Fernandes, B. Colaço, A. Gama, M. C. Paiva, P. S. Gomes, R. F. Silva and M. H. Fernandes, *Nanoscale*, 2015, **7**, 9238–9251.
17 V. E. Kagan, N. V. Konduru, W. Feng, B. L. Allen, J. Conroy, Y. Volkov, I. I. Vlasova, N. A. Belikova, N. Yanamala and A. Kapralov, *Nat. Nanotechnol.*, 2010, **5**, 354–359.
18 I. Vlasova, A. Sokolov, A. Chekanov, V. Kostevich and V. Vasilyev, *Russ. J. Bioorg. Chem.*, 2011, **37**, 453–463.
19 N. Lu, J. Li, R. Tian and Y.-Y. Peng, *Chem. Res. Toxicol.*, 2014, **27**, 1070–1077.
20 P. W. Rose, A. Prlić, C. Bi, W. F. Bluhm, C. H. Christie, S. Dutta, R. K. Green, D. S. Goodsell, J. D. Westbrook and J. Woo, *Nucleic Acids Res.*, 2015, **43**, D345–D356.
21 G. I. Berglund, G. H. Carlsson, A. T. Smith, H. Szöke, A. Henriksen and J. Hajdu, *Nature*, 2002, **417**, 463–468.

22 A. Singh, N. Singh, S. Sharma, K. Shin, M. Takase, P. Kaur, A. Srinivasan and T. Singh, *Biophys. J.*, 2009, **96**, 646–654.
23 D. Schneidman-Duhovny, Y. Inbar, R. Nussinov and H. J. Wolfson, *Nucleic Acids Res.*, 2005, **33**, W363–W367.
24 E. Mashiach, D. Schneidman-Duhovny, N. Andrusier, R. Nussinov and H. J. Wolfson, *Nucleic Acids Res.*, 2008, **36**, W229–W232.
25 G. A. Kaminski, R. A. Friesner, J. Tirado-Rives and W. L. Jorgensen, *J. Phys. Chem. B*, 2001, **105**, 6474–6487.
26 H. J. Berendsen, J. P. Postma, W. F. van Gunsteren and J. Hermans, in *Intermolecular forces*, Springer, 1981, pp. 331–342.
27 B. Hess, C. Kutzner, D. Van Der Spoel and E. Lindahl, *J. Chem. Theory Comput.*, 2008, **4**, 435–447.
28 T. Paramo, A. East, D. Garzón, M. B. Ulmschneider and P. J. Bond, *J. Chem. Theory Comput.*, 2014, **10**, 2151–2164.
29 G. P. Kotchey, Y. Zhao, V. E. Kagan and A. Star, *Adv. Drug Delivery Rev.*, 2013, **65**, 1921–1932.
30 B. L. Allen, G. P. Kotchey, Y. Chen, N. V. Yanamala, J. Klein-Seetharaman, V. E. Kagan and A. Star, *J. Am. Chem. Soc.*, 2009, **131**, 17194–17205.
31 F. T. Andón, A. A. Kapralov, N. Yanamala, W. Feng, A. Baygan, B. J. Chambers, K. Hultenby, F. Ye, M. S. Toprak and B. D. Brandner, *Small*, 2013, **9**, 2721–2729.
32 G. Modugno, F. Ksar, A. Battigelli, J. Russier, P. Lonchambon, E. Eleto da Silva, C. Ménard-Moyon, B. Soula, A.-M. Galibert, M. Pinault, E. Flahaut, M. Mayne-L'Hermite and A. Bianco, *Carbon*, 2016, **100**, 367–374.
33 M. Chen, X. Qin, J. Li and G. Zeng, *RSC Adv.*, 2016, **6**, 3592–3599.
34 H. Shams, B. D. Holt, S. H. Mahboobi, Z. Jahed, M. F. Islam, K. N. Dahl and M. R. K. Mofrad, *ACS Nano*, 2014, **8**, 188–197.
35 S. Saha, T. C. Dinadayalane, J. S. Murray, D. Leszczynska and J. Leszczynski, *J. Phys. Chem. C*, 2012, **116**, 22399–22410.
36 M. Monajjemi, R. Faham and F. Mollaamin, *Fullerenes, Nanotubes, Carbon Nanostruct.*, 2012, **20**, 163–169.
37 Y. Li and M. Kröger, *Carbon*, 2012, **50**, 1793–1806.
38 B. Luan, T. Huynh, L. Zhao and R. Zhou, *ACS Nano*, 2015, **9**, 663–669.
39 M. Feng, H. Kang, Z. Yang, B. Luan and R. Zhou, *J. Chem. Phys.*, 2016, **144**, 225102.
40 F. Tavanti, A. Pedone and M. C. Menziani, *J. Phys. Chem. C*, 2015, **119**, 22172–22180.
41 M. Calvaresi, S. Hoefinger and F. Zerbetto, *Chem. – Eur. J.*, 2012, **18**, 4308–4313.
42 T. Chang, J. Geng and X. Guo, *Appl. Phys. Lett.*, 2005, **87**, 251929.
43 R. B. Capaz, C. D. Spataru, S. Ismail-Beigi and S. G. Louie, *Phys. Rev. B: Condens. Matter Mater. Phys.*, 2006, **74**, 121401.
44 S. Manzetti, O. Andersen, C. Garcia and E. Campos, *Mol. Simul.*, 2016, 1–10.
45 X. Zhao, D. Lu, F. Hao and R. Liu, *J. Hazard. Mater.*, 2015, **292**, 98–107.